OPTIMAL TUNING OF PI-CONTROLLER OF SHUNT ACTIVE POWER FILTER FOR HARMONICS MITIGATION USING ENHANCED JUMPING SPIDER ALGORITHM

Betrand N. **ATANGA**, Francis B. **EFFAH,** Daniel **KWEGYIR,** Philip Y. **OKYERE**
Kwame Nkrumah University of Science and Technology, Kumasi, Ghana
atangabertrand@gmail.com, fbeffah74@gmail.com

Keywords: shunt active power filter, PI-controller, harmonics mitigation, p-q theory

Abstract*: The increasing use of power electronic devices has resulted in harmonics that may cause in power systems overheating of equipment, poor power factor and voltage distortion. Shunt active power filter (SAPF) provides the most useful means for harmonics mitigation in power systems. In a certain number of SAPFs, the dc link capacitor voltage is regulated by means of a PI controller. This paper proposes a variant of a population based Jumping Spider Algorithm for optimal tuning of the PI controller to enhance the performance of the active filter. The SAPF considered in this paper uses the p-q theory to extract its reference current and the hysteresis current control to produce the triggering signals for the controlled switching devices of its inverter. The overall SAPF is developed and validated using MATLAB/Simulink tool under two different nonlinear loading conditions. The results obtained by simulation show that the SAPF with the proposed PI controller effectively controls the dc-link capacitor voltage and mitigates current harmonics.*

1. INTRODUCTION

Nowadays, there is an increased use of nonlinear loads such as computers, microwave oven, adjustable electric drives and arc furnaces in both domestic and industrial applications. These nonlinear loads give rise to current harmonics which cause power losses, overheating of equipment, and premature damage to motors, cables, transformers and sensitive equipment [1]. The Shunt Active Power Filter (SAPF) is preferred for reducing harmonics, compensating

for reactive power and improving power factor. The widely used SAPF consists of voltage fed or voltage source inverter (VSI) and its controller. The controller performs four main control actions [2], namely the extraction of harmonic currents or generation of reference current, control of dc link capacitor voltage, current control and synchronization. In some controllers, synchronization action is not explicitly required. The efficient performance of SAPF largely depends on the effectiveness of its control techniques [3].

The contribution of this paper is in the area of dc-link capacitor voltage control. The conduction and switching losses in the VSI cause a drop in the value of the capacitor voltage which then adversely affects the compensation performance of the active power filter [4]. Therefore, the capacitor voltage is regulated to keep it constant. The most common approach to regulate the capacitor voltage is the use of PI controller [5]. Conventional PI controller may not give optimum solution, because they require precise linear models. Again, the PI controller underperforms in the presence of non-linear loads, parameter variation, and disturbance [6]

Recently, researchers have used metaheuristic algorithms-based optimization techniques such as PSO [7], Ant Colony (ACO) [8], Genetic Algorithm (GA) [9], Bacteria Foraging [10], artificial bee colony (ABC) [11], to find the optimum gains of the PI controller of SAPF. None of these techniques seems to have yielded optimal parameters for the PI controller [12] and as one particular meta-heuristic algorithm is not capable of producing good results in all fields, researchers continue to try with new ones. This paper presents a new metaheuristic algorithm known as Enhanced Jumping Spider Algorithm (EJSA) for finding the optimum gains of the PI controller of the SAPF. The paper is organized as follows, section 2 – Theoretical background, section 3 – Implementation, section 4 – Results and discussions, and section 5 – Conclusion.

2. THEORITICAL BACKGROUND

2.1. SAPF Configuration and operation

A shunt active power filter has two main components, namely the power component and the control component. The power component consists of a VSI, an energy storage dc link capacitor, which maintains DC voltage at the VSI input, and an inductor which connects the VSI to the power system and acts as a filter. The function of the power component is to inject the needed mitigating current.

The SAPF works as follows. The power system's current in the absence of the filter at the point of common coupling (PCC) can be expressed as:

$$i_S = i_L = i_{1L} + i_H \tag{1}$$

where i_s = supply current, i_L = load current, and i_{1L} = fundamental component of the load current and i_H = harmonics present in the load current.

A SAPF connected to the PCC introduces these additional currents: the compensating current i_C injected by the SAPF which is equal and opposite in phase to i_H and then the dc link current i_{dc} drawn by the SAPF to account for the losses occurring in its switching devices and to keep the dc link capacitor voltage constant. The source current then becomes:

$$i_S = i_L = [i_{1L} + i_H] - i_C + i_{dc} \tag{2}$$

Harmonics mitigation current is obtained through the dc link capacitor voltage. By maintaining this voltage at a preset level, the compensation current becomes inversely identical to the harmonic component of the non-linear loads, thereby cancelling out each other. The source then supplies sinusoidal current having the fundamental frequency [2]. Equation (2) now becomes:

$$i_S = i_{1L} + i_{dc} \tag{3}$$

The SAPF controller continuously monitors the harmonics in the source current, which varies with time and then commands the power circuit to inject the necessary mitigating current.

2.2. Harmonic extraction algorithm

Harmonic extraction algorithm generates a reference current from the distorted load current. It is considered to be the most important control action [13]. The existing techniques that can be used to generate the reference current are many. The p-q theory, one of the most widely used time-domain techniques, is used in this work. These techniques require simple and less calculations and therefore, reduce the control process time. It does not require synchronization algorithm such as phase-lock loop technique, which involves complex calculations [2]. The p-q theory uses Clark transformation to convert currents and voltages from abc frame representation to 0αβ frame representation as follows:

$$\begin{bmatrix} i_0 \\ i_\alpha \\ i_\beta \end{bmatrix} = \sqrt{\frac{2}{3}} \cdot \begin{bmatrix} 1/\sqrt{2} & 1/\sqrt{2} & 1/\sqrt{2} \\ 1 & -1/2 & -1/2 \\ 0 & \sqrt{3}/2 & \sqrt{3}/2 \end{bmatrix} \cdot \begin{bmatrix} i_a \\ i_b \\ i_c \end{bmatrix} \tag{4}$$

$$\begin{bmatrix} v_0 \\ v_\alpha \\ v_\beta \end{bmatrix} = \sqrt{\frac{2}{3}} . \begin{bmatrix} \frac{1}{\sqrt{2}} & \frac{1}{\sqrt{2}} & \frac{1}{\sqrt{2}} \\ 1 & -\frac{1}{2} & -\frac{1}{2} \\ 0 & \frac{\sqrt{3}}{2} & \frac{\sqrt{3}}{2} \end{bmatrix} . \begin{bmatrix} v_a \\ v_b \\ v_c \end{bmatrix} \quad (5)$$

where i_a, i_b, and i_c are three-phase currents and v_a, v_b, and v_c are three-phase voltages in abc frame, and i_0, i_α and i_β are three-phase currents and v_0, v_α, and v_β are three-phase voltages in 0αβ frame.

For a three-phase, three-wire supply system considered in this paper, the zero-sequence component is absent. The instantaneous complex power *s* in the 0αβ frame is given by:

$$S = p + jq = v_{\alpha\beta} i^*_{\alpha\beta} = \left(v_\alpha - jv_\beta\right)\left(i_\alpha + ji_\beta\right) = \left(v_\alpha i_\alpha + v_\beta i_\beta\right) + j(v_\alpha i_\beta - v_\beta i_\alpha) \quad (6)$$

where p = instantaneous active power and q = instantaneous reactive power. The symbol "$*$ " denotes conjugate.

The p and q can be restated in the matrix form as follows:

$$\begin{bmatrix} p \\ q \end{bmatrix} = \begin{bmatrix} v_\alpha & v_\beta \\ -v_\beta & v_\alpha \end{bmatrix} . \begin{bmatrix} i_\alpha \\ i_\beta \end{bmatrix} \quad (7)$$

where nonlinear loads are present, p can be expressed as the sum of AC and DC components as follows:

$$p = \bar{p} + \tilde{p} \quad (8)$$

The component $\bar{p}$ is the DC component or average of p. It represents the power due to the fundamental voltages and currents and corresponds to the power drawn by the load from the source. The component $\tilde{p}$ is the AC component of p and represents the energy that flows to and from the load and the source. The harmonic reference current is calculated from $\tilde{p}$ and q after $\bar{p}$ has been extracted by a low pass filter.

If the power absorbed by the SAPF to account for losses in the switching devices to keep the capacitor voltage constant is denoted by $\tilde{P}_{loss}$ then the ac component of the instantaneous real power is calculated as follows:

$$\tilde{p} = P - \bar{p} - \tilde{P}_{loss} \quad (9)$$

The reference supply currents in αβ-frame (i^*_α, i^*_β) are then obtained by (10) and are further transformed to the *abc*-frame (i^*_a, i^*_b, i^*_c) through the inverse Clarke's transformation by (11).

$$\begin{bmatrix} i_\alpha^* \\ i_\beta^* \end{bmatrix} = \frac{1}{V_\alpha^2+V_\beta^2} \cdot \begin{bmatrix} v_\alpha & -v_\beta \\ v_\beta & v_\alpha \end{bmatrix} \cdot \begin{bmatrix} \tilde{p} \\ Q \end{bmatrix} \quad (10)$$

$$\begin{bmatrix} i_a^* \\ i_b^* \\ i_c^* \end{bmatrix} = \sqrt{\frac{2}{3}} \cdot \begin{bmatrix} 1 & 0 \\ -1/2 & \sqrt{3}/2 \\ -1/2 & -\sqrt{3}/2 \end{bmatrix} \cdot \begin{bmatrix} i_\alpha^* \\ i_\beta^* \end{bmatrix} \quad (11)$$

Figure 1 is a block diagram showing how reference current is generated using the p-q theory [14].

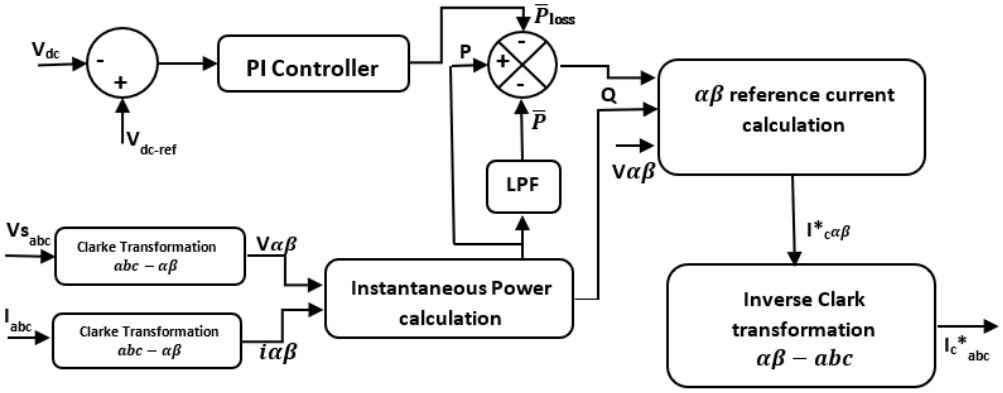

Fig. 1. Block diagram of reference current generation by p-q theory

2.3. Hysteresis Current Control Technique

The hysteresis current control technique is employed to produce the VSI triggering signals in such a way that its output current will have a wave shape identical but opposite in phase to that of the reference current. This paper uses the hysteresis current control technique which is the most widely used technique because of its fast response, accuracy, assured stability and easy implementation [15]. In this technique, the current produced by the inverter I_{fabc} is kept in a hysteresis band around the reference current I_{rabc}. The controller compares the two currents and, based on the error, outputs appropriate switching pulses to the VSI so that the filter current I_{fabc} is maintained inside a hysteresis band [16].

2.4. Algorithm for Regulating dc link Capacitor Voltage

In SAPF, it is important to keep the DC side of the voltage fed inverter constant by controlling the capacitor voltage. Ideally, the capacitor voltage should remain constant and the filter should not draw active power from the power system. This is, however, not the case because conduction and switching losses occur in the VSI during its operation [2]. Most SAPFs use a PI controller to regulate the capacitor voltage because it is simple to implement. The

measured capacitor voltage $v_{dc}$and the desired reference voltage V_{dc_ref} are compared and the corresponding error $e(t)$ is used to feed the PI controller. The PI controller output current is given by:

$$i_{dc} = K_p e(t) + K_i \int_0^t e(t)dt \tag{12}$$

where $e(t)$, the dc-link capacitor voltage error, is defined as

$$e(t) = V_{dc\_ref} - V_{dc} \tag{13}$$

with V_{dc}= the measured capacitor voltage and V_{dc_ref}= the reference capacitor voltage.

This current is used to adjust the reference current so that the right amount of real power will be absorbed by the filter to account for its conduction and switching losses [2].

This paper uses EJSOA to obtain the optimum gain parameters of the PI controller with its fitness or objective function defined as the integral time absolute error (ITAE). The ITAE performance index, the preferred criterion when designing this controller [17], is given by

$$J = \int_0^T t\,|e(t)|dt \tag{14}$$

2.4.1. Enhanced Jumping Spider Optimization Algorithm (EJSOA)

EJSO is a novel and simple meta-heuristic algorithm which mimics the hunting strategies of a jumping spider. A random population of spiders is initially produced to catch a prey in a multidimensional space. The spiders are deemed to use three hunting strategies, namely search for prey, consisting of local search and global search, attack by persecution and attack by jumping on prey[18]. The local search is described by the equation:

$$\vec{x}_i(k+1) = \vec{x}_{best}(k) + walk\left(\frac{1}{2} - \varepsilon\right) \tag{15}$$
$$i = 1, 2, 3, \dots, n.$$

where $\vec{x}_i(k+1)$ = the *i*th spider new position, $\vec{x}_{best}(k)$ = best location of spiders from previous iteration, $walk$ = a uniformly distributed random number generated in the interval [-2, 2] and ε = a randomly generated number in the interval [0,1].

The Lévy flight is applied for the global search. It is given by:

$$\vec{x}_i(k+1) = \vec{x}_{best}(k) + \gamma . L_\alpha(S) \tag{16}$$

where $\vec{x}_i(k+1)$ = the *i*th spider new position and γ ($\gamma > 0$) = the step size, $L_\alpha(S)$ gives a random walk with a random step length *S*. The search ability is most affected by the value of α [19]. A value of 1.5 is usually used.

Attack by persecution represents the situation where a spider is not close enough to the prey and it has to crawl close to the prey before it jumps on it. This walk is represented by:

$$\vec{x}_i(k+1) = \frac{1}{2}\left(\vec{x}_i(k) - \vec{x}_r(k)\right) \tag{17}$$

where $\vec{x}_i(k+1)$ = the *i*th spider new position, $\vec{x}_i(k)$ = the *i*th spider position in the preceding iteration, and $\vec{x}_r(k)$ = the position of spider r ($r \neq i$) randomly selected from the preceding iteration.

In the case of attack by jumping on prey, the spider is close to the prey so it jumps on it. The jump is modelled by:

$$\vec{x}_i(k+1) = \left(\vec{x}_i(k)\, tan(\alpha) - \frac{g\vec{x}_i^2(k)}{2V_0^2 cos^2(\alpha)}\right) * \mu \tag{18.a}$$

$$\alpha = \frac{\varphi\pi}{180} \tag{18.b}$$

where $\vec{x}_i(k+1)$ = the *i*th spider new position and $\vec{x}_i(k)$ = the *i*th spider current position. Both φ (in degress) and μ are random numbers produced in the interval (0, 1). V_o = the speed of the spider projection and g = acceleration duet o gravity. V_o, = 100 mm/sec and g = 9.80665 m/s^2..

The fitness values of search agents are normalized. The normalized value called pheromone is calculated as follows:

$$pheromone(i) = \frac{Fitness_{max} - Fitness(i)}{Fitness_{max} - Fitness_{min}} \tag{19}$$

where *Fitness(i)* = the *i*th spider current fitness value and $Fitness_{max}$ = the best fitness value of the current generation and $Fitness_{min}$ = the worst value of the current generation. The maximum pheromone value, the best value, is 1 and the minimum pheromone value, the worst value, is 0.

If a spider has its pheromone value ≤ 0.3, its position is updated as follows:

$$\vec{x}_i(k) = \vec{x}_{best}(k) + \frac{1}{2}\left(\vec{x}_{r1}(k) - (-1)^\sigma * \vec{x}_{r2}(k)\right) \tag{20}$$

$$r_1 \neq r_2$$

where $\vec{x}_{r1}(k)$ and $\vec{x}_{r2}$ are the positions of spiders r_1 and r_2 which are randomly selected, $\vec{x}_{best}(k)$ is the best position of the spiders in the preceding iteration and σ is a binary number selected at random from 0 and 1.

The EJSO algorithm is represented by the flow chart shown in *fig. 2*.

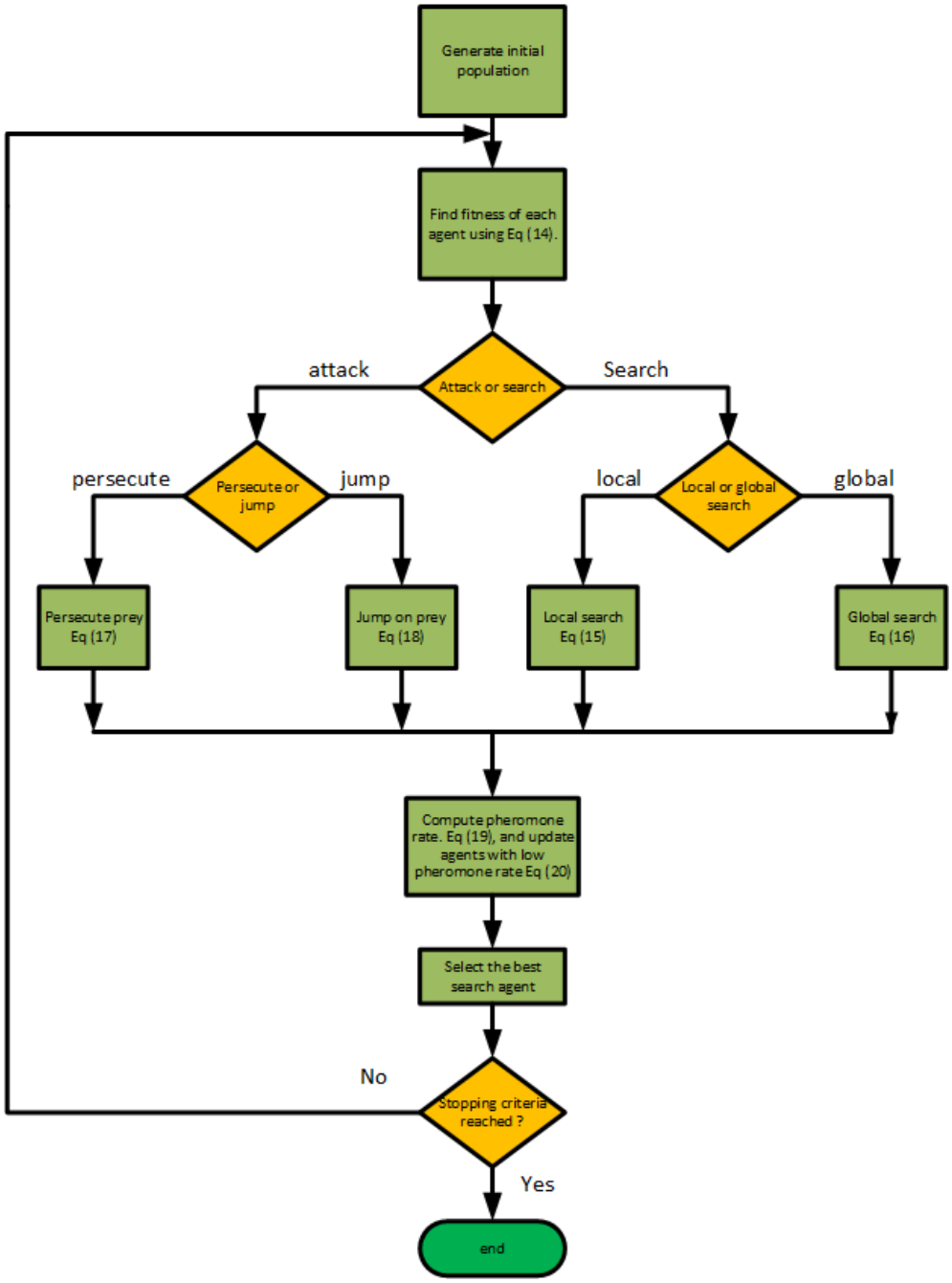

Fig. 2. Flowchart of Jumping Spider Algorithm [18]

2.4.2. Tuning of PI Controller with EJSOA

The following steps are taken to obtain optimum tuning values of the PI controller using EJSOA:

1. Build the SAPF model including the controller algorithms in Simulink.
2. Set parameters of the SAPF.
3. Set initial parameters of EJSOA (i.e., population size (*N*), dimension (*D*), maximum number of iteration)

4. Generate initial random population of spiders ($S_i = 1, 2, \ldots, N$) with dimension $D = 2$ (representing K_p and K_i)
5. Run the SAPF model for a specified nonlinear load using the initial K_p and K_i values and calculate the initial fitness of spiders S_{fit} using (14) for a specified T and sampling rate τ
6. **While** iteration < maximum number of iterations **do**
   if random number generated < 0.5 **then** Attack
   if random number generated < 0.5 **then**
   It is Attack by persecution. Use (17)
   else
   It is Attack by jumping on the prey. Use (18)
   end if
   else Search
   if random number generated < 0.5 **then**
   It is local search for prey. Use (15)
   else
   It is global search for prey. Use (16)
   end if
   end if
7. Calculate pheromone rate using (19)
8. Update search agents' positions (K_p and K_i) that have low pheromone rate using (20)
9. Run the SAPF model and calculate the new fitness of spiders $S_{fit,new}$ using (14)
10. **if** $S_{fit,new} < S_{fit}$ **then**
11. set $S_{fit} = S_{fit,new}$
12. **end if**
13. iteration =iteration + 1
14. **end while**
15. Output the best K_p and K_i values

3. IMPLEMENTATION

MATLAB/Simulink tool has been used to determine how effective the proposed PI controller is in mitigating current harmonics. *Figure 3* shows the complete Simulink models of the power and control blocks. The power blocks comprise the following three components: a three-phase, three-wire voltage source, a nonlinear load consisting of a three-phase uncontrolled rectifier feeding a passive load and a shunt active power filter. The shunt active power filter comprises a dc-bus capacitor, six-IGBT switches with diodes.

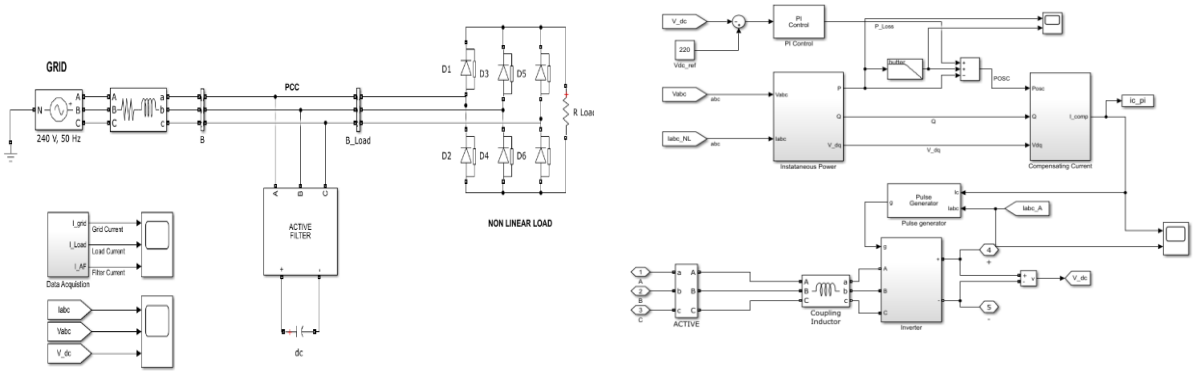

(a) Power Blocks *(b) Control Blocks*

Fig.3. MATLAB/Simulink Model of SAPF

3.1. Optimal tuning of the PI controller

The EJSOA parameters used for finding the optimum tuning values of the PI controller are presented in Table 1. The parameters of the power system, the SAPF and the nonlinear load are given in Table 2 and the complete Simulink model of the control circuit with ITAE block is shown in *fig. 4.*

Table 1. Parameters of EJSOA for optimal tuning

Parameters	**Values**
Population size	50
Number of iterations	30
Sampling period T	1
Sampling rate τ	0.005 ms

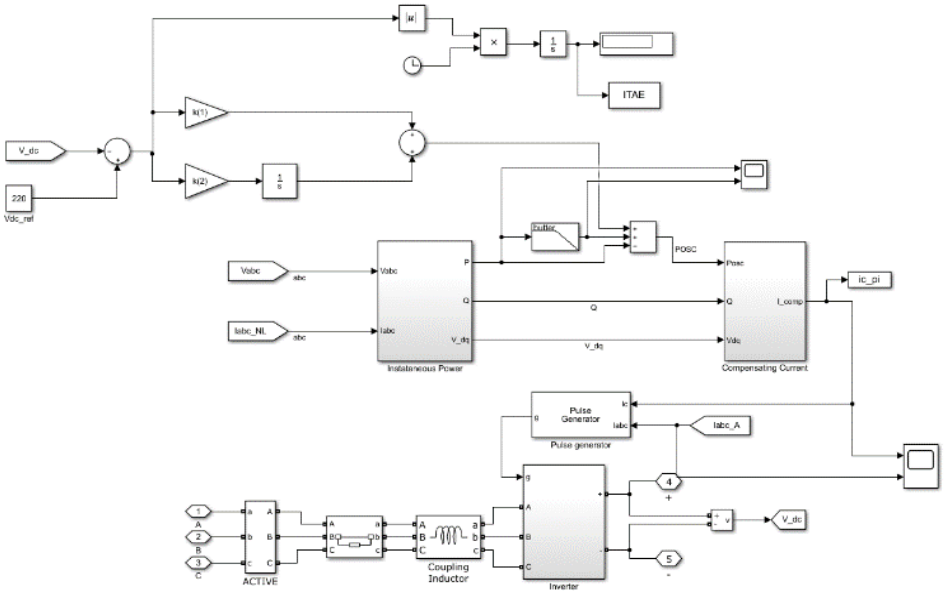

Fig. 4. Simulink model with ITAE block

Table 2. Parameters of overall system for optimal tuning

Parameters	**Values**
Source voltage	380 V
frequency	50 Hz
Line inductor	L_s = 10 mH
Filter inductor	L_f = 0.15 mH
DC-link capacitor	C = 1000 μF
DC load resistance	50 Ω
DC link capacitor voltage	600 V

3.2. Testing

After finding the optimum tuning values of the PI controller, the performance of the proposed SAPF was evaluated using dc load resistances of 50 ohms and 25 ohms. The 50-ohm load resistance is the same as what was used for the optimal tuning of the PI controller. The constants of the power system and the SAPF are as defined in Table 2. The Simulink model of the control blocks used for testing the proposed system is the same as that given in Fig. 4 without the ITAE block.

4. RESULTS AND DISCUSSIONS

4.1. Optimal tuning values of PI controller

The optimal gains obtained were: K_p = 0.057175 and K_i = -1. These gains were then used to verify the effectiveness of the proposed PI controller. Two dc resistances were considered. These two gain values and other system parameters were maintained for the two dc resistance loads.

4.1.1. Source Current Waveform and its Harmonic Spectrum

Case 1: DC resistance = 50 Ω

Figure 5(a) and *fig. 5(b)* show the source current waveform and its harmonic spectrum before connecting the SAPF.

Figures 6(a) and *6(b)* show the corresponding curves when the SAPF is in circuit. From the FFT analysis, the THD reduces from 26.12% to 0.55%.

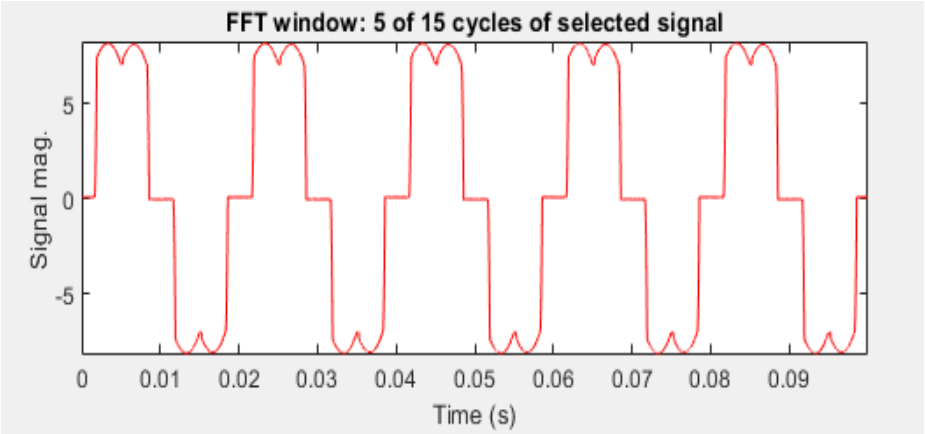

(a) Waveform of source current

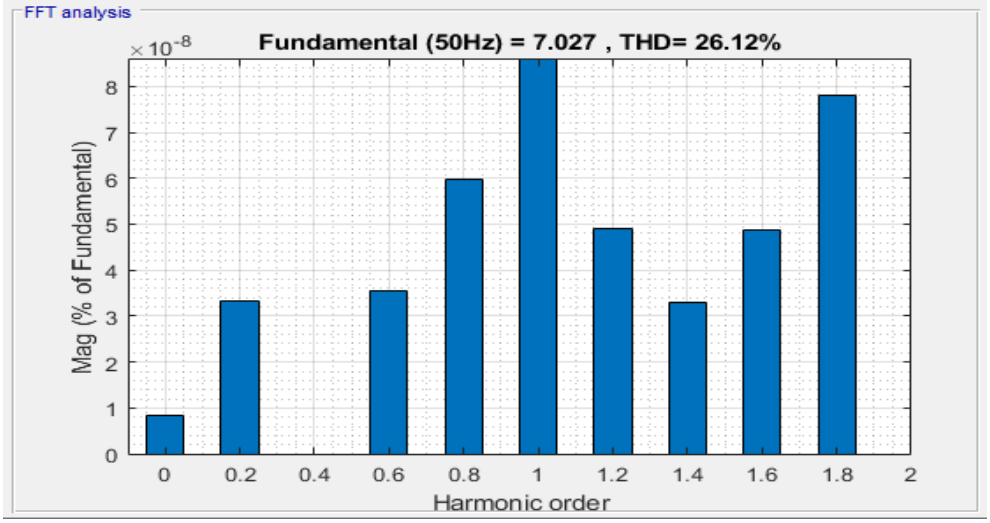

(b) Source current harmonc spectrum

Fig. 5. Source current before compensation

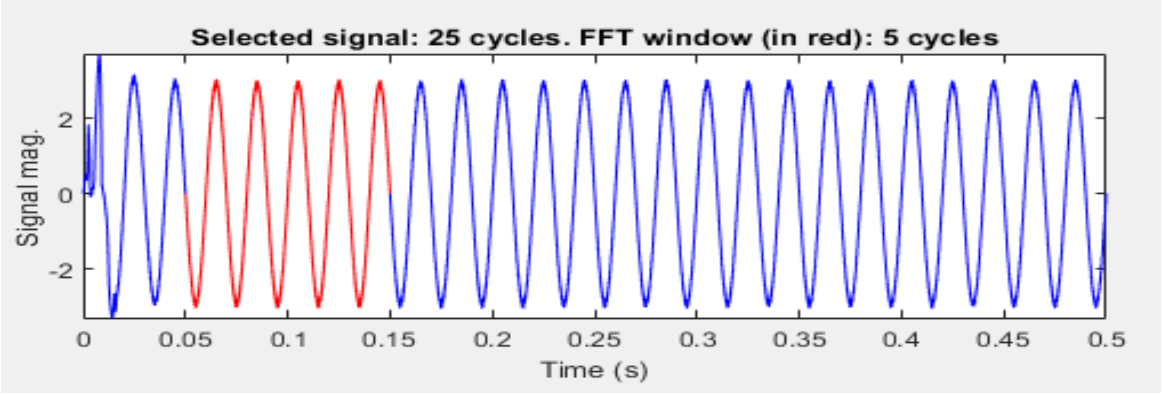

(a) Waveform of source current

Fig. 6. Source current after compensation

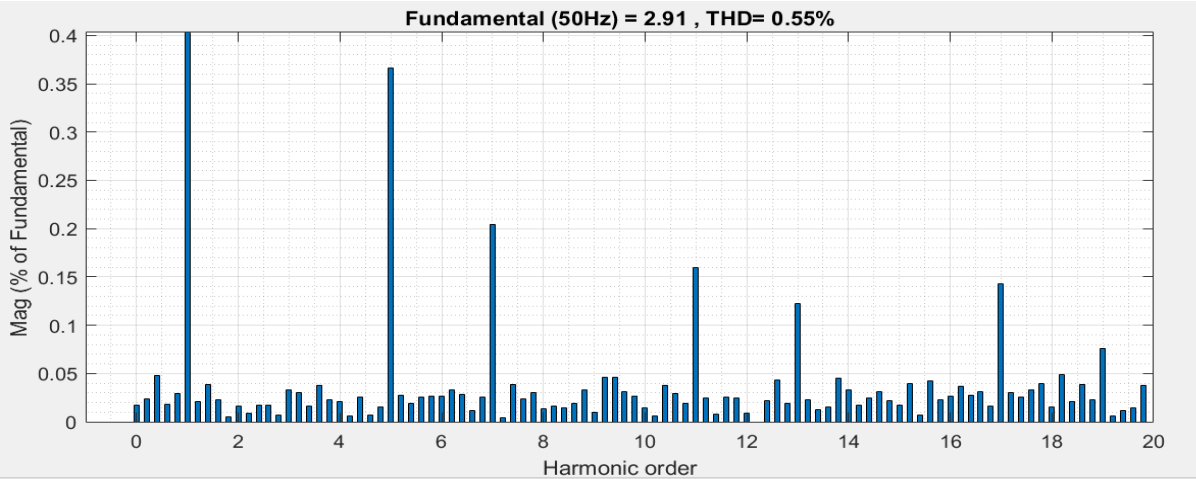

(b) Supply current harmonic spectrum

Fig. 6. Source current after compensation

Case 2: DC resistance = 25 Ω

Figure 7(a) and *fig.7(b*) show the source current waveform and its harmonic spectrum before connecting the SAPF.

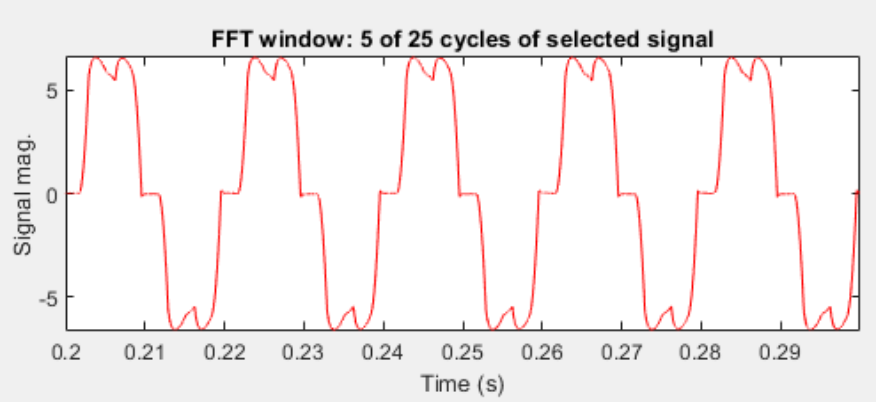

(a) Waveform of source current

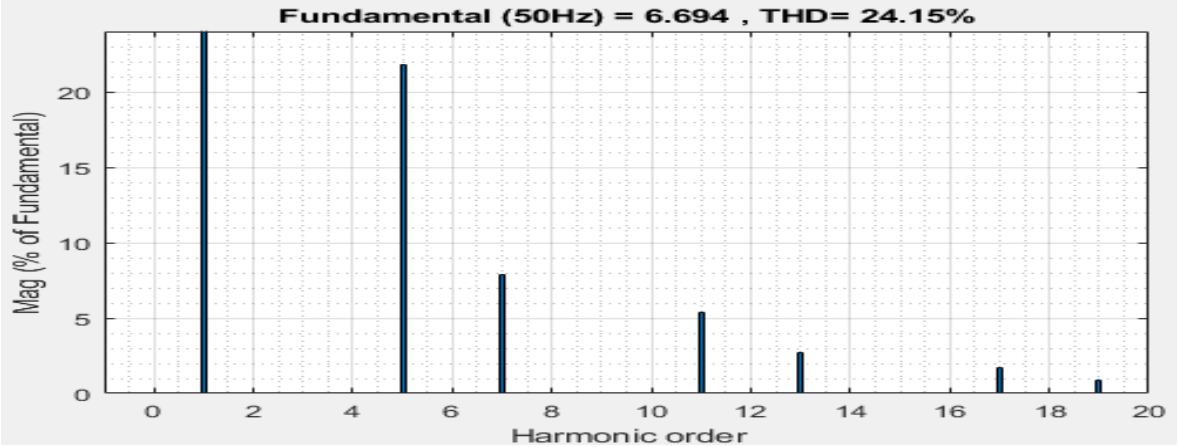

(b) Source current harmonic spectrum

Fig. 7. Source current before compensation

Figures 8(a) and *8(b)* show the corresponding curves when the SAPF is connected. The FFT analysis shows a reduction of the THD from 24.15% to 0.53%.

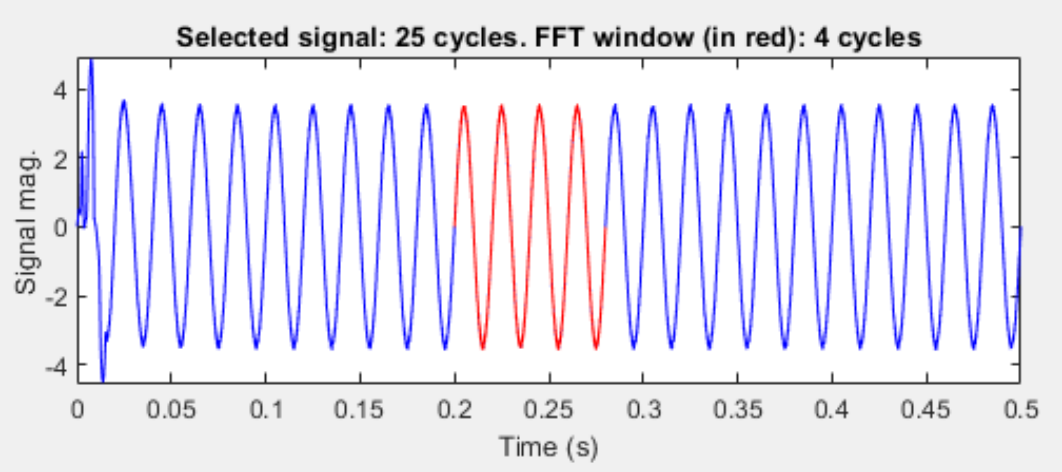

(a) Waveform of source current

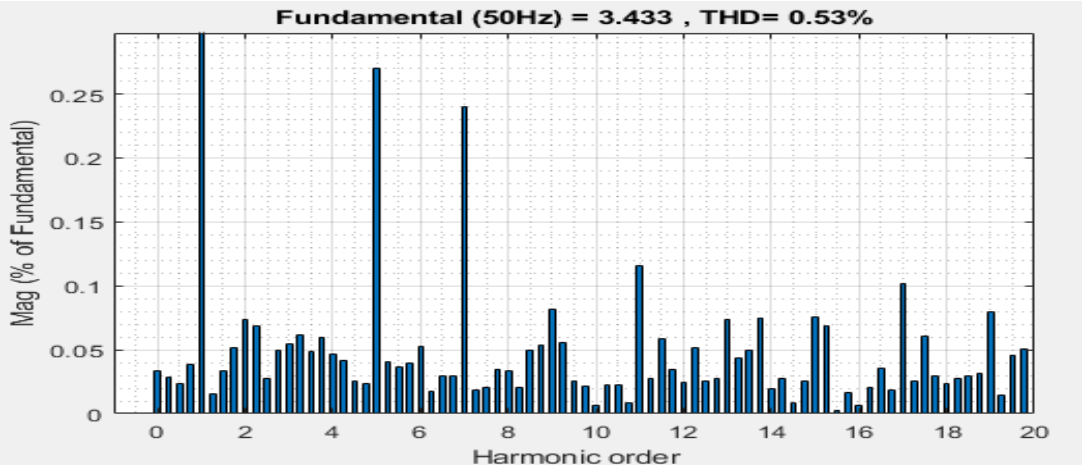

(b) Source current harmonic spectrum

Fig. 8. Source current after compensation

4.2. DC link capacitor voltage response

Figure 9 shows the response of the dc link capacitor voltage regulated by the proposed PI controller for the 50-ohm dc resistance load. The corresponding response for the 25-ohm dc resistance loads is shown in Fig.10. The two waveforms show a fast and stable response with zero steady-state error. Each of the waveforms also has an overshoot of about 17% which makes the response fast. *Figure 11* gives the waveform for the case where the SAPF was run with initial dc resistance load of 50 ohms and at t = 0.25s the dc resistance load was suddenly decreased to 25 ohms to double the load current. As shown by the waveform, the voltage across the capacitor dropped when the current drawn by the load suddenly doubled but it quickly recovered.

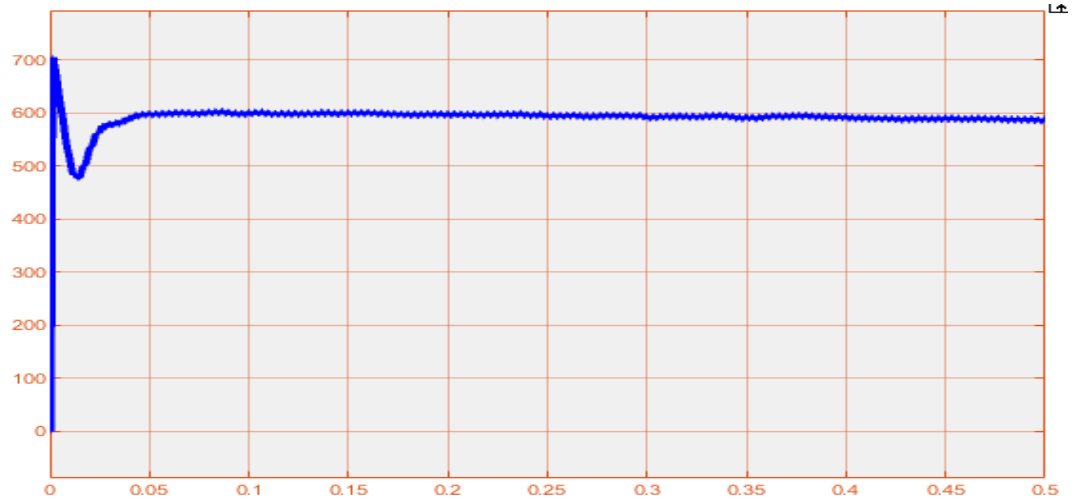

Fig. 9. SAPF capacitor voltage 50-ohm dc load resistance

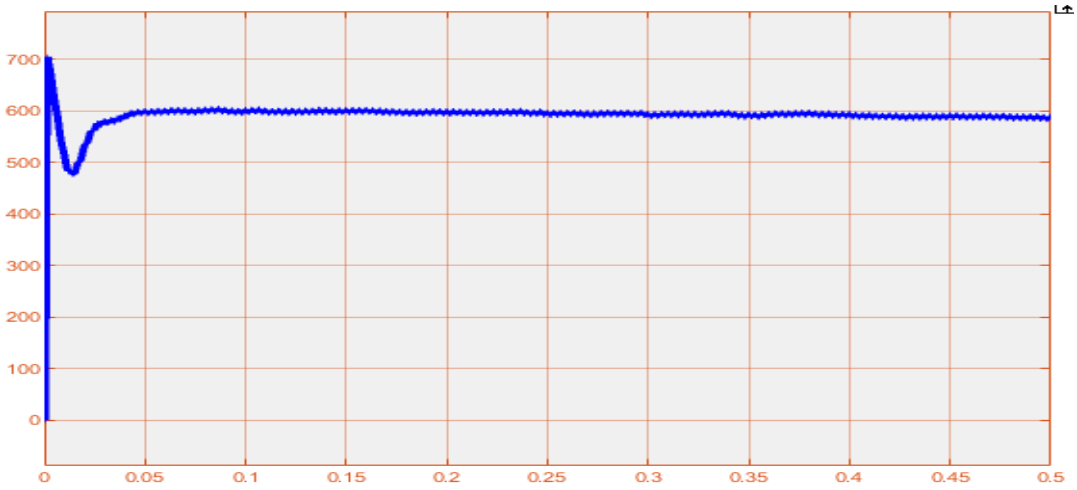

Fig.10. SAPF capacitor voltage for 25-ohm dc resistance

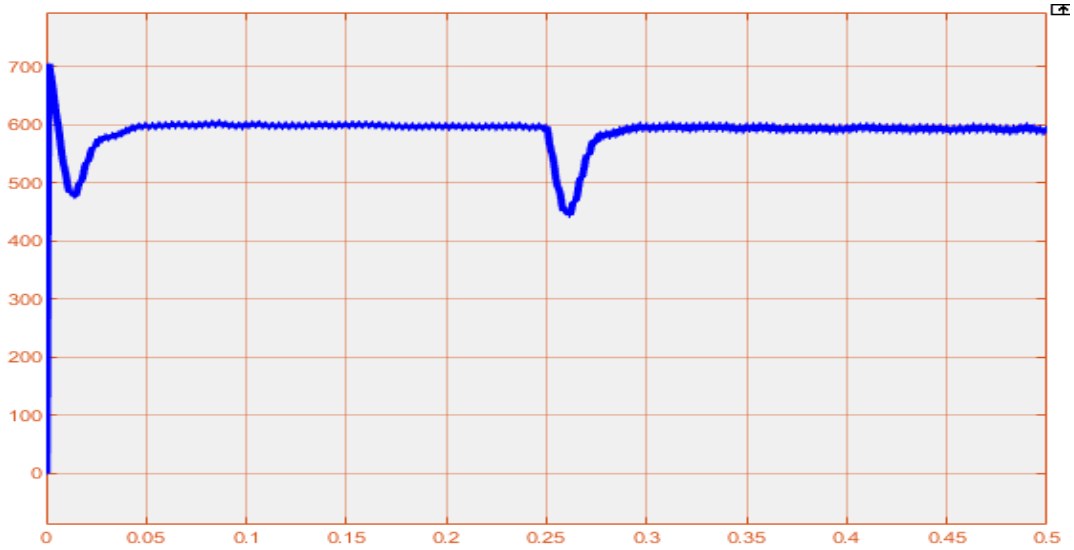

Fig.11. SAPF capacitor voltage when load current doubles.

5. CONCLUSION

The EJSOA has been applied to optimally tune the PI controller of SAPF to mitigate harmonics in power systems. The PI controller has been used for the regulation of the dc link capacitor voltage of the SAPF. The EJSOA has employed the ITAE as the fitness function to determine the optimum gains of the PI Controller. SAPF using this PI controller has been developed and simulated in MATLAB/Simulink environment. The EJSOA-PI controller produced a dc link capacitor voltage response that is fast, stable and steady-state error-free. The capacitor voltage also recovers quickly when it drops in value following a sudden variation in load. The results also showed that the SAPF with the EJSOA-PI controller is capable of reducing the THD of a balanced power system from 26.12% to 0.53%, a figure which is far below the IEEE harmonic standard limit of 5%.

REFERENCES

[1] A. E. S. Salem, O. M. Salim, and S. I. Arafa, *New triple-action controller for inverter power quality improvement*, Comput. Electr. Eng., vol. 81, 2020, doi: 10.1016/j.compeleceng.2019.106543.

[2] Y. Hoon, M. A. M. Radzi, M. K. Hassan, and N. F. Mailah, *Control algorithms of shunt active power filter for harmonics mitigation:* A review, Energies, vol. 10, no. 12, 2017, doi: 10.3390/en10122038.

[3] Y. Hoon, M. A. M. Radzi, M. K. Hassan, N. F. Mailah, and N. I. A. Wahab, *A simplified synchronous reference frame for indirect current controlled three-level inverter-based shunt active power filters*, J. Power Electron., vol. 16, no. 5, pp. 1964–1980, 2016, doi: 10.6113/JPE.2016.16.5.1964.

[4] R. R. Nasyrov, R. I. Aljendy, and A. A. Z. Diab, *Adaptive PI controller of active power filter for compensation of harmonics and voltage fluctuation based on particle swarm optimization (PSO)*, Proc. 2018 IEEE Conf. Russ. Young Res. Electr. Electron. Eng. ElConRus 2018, vol. 2018-Janua, pp. 719–724, 2018, doi: 10.1109/EIConRus.2018.8317194.

[5] A. Fereidouni and M. A. S. Masoum, *Enhancing performance of active power filter with fuzzy logic controller using adaptive hysteresis direct current control*, 2014 Australas. Univ. Power Eng. Conf. AUPEC 2014 - Proc., no. October, pp. 1–6, 2014, doi: 10.1109/AUPEC.2014.6966500.

[6] S. Mahaboob, S. K. Ajithan, and S. Jayaraman, *Optimal design of shunt active power filter for power quality enhancement using predator-prey based firefly optimization*, Swarm Evol. Comput., vol. 44, no. June 2018, pp. 522–533, 2019, doi: 10.1016/j.swevo.2018.06.008.

[7] D. Tian and Z. Shi, MPSO: *Modified particle swarm optimization and its applications*, Swarm Evol. Comput., vol. 41, pp. 49–68, 2018, doi: 10.1016/j.swevo.2018.01.011.

[8] H. Ismkhan, *Effective heuristics for ant colony optimization to handle large-scale problems*, Swarm Evol. Comput., vol. 32, pp. 140–149, 2017, doi: 10.1016/j.swevo.2016.06.006.

[9] Q. Long, *A constraint handling technique for constrained multi-objective genetic algorithm*, Swarm Evol. Comput., vol. 15, pp. 66–79, 2014, doi: 10.1016/j.swevo.2013.12.002.

[10] T. Sudhakar Babu, K. Priya, D. Maheswaran, K. Sathish Kumar, and N. Rajasekar, *Selective voltage harmonic elimination in PWM inverter using bacterial foraging algorithm*, Swarm Evol. Comput., vol. 20, pp. 74–81, 2015, doi: 10.1016/j.swevo.2014.11.002.

[11] R. Akbari, R. Hedayatzadeh, K. Ziarati, and B. Hassanizadeh, *A multi-objective artificial bee colony algorithm*, Swarm Evol. Comput., vol. 2, pp. 39–52, 2012, doi: 10.1016/j.swevo.2011.08.001.

[12] K. Rameshkumar and V. Indragandhi, *Real Time Implementation and Analysis of Enhanced Artificial Bee Colony Algorithm Optimized PI Control algorithm for Single Phase Shunt Active Power Filter*, J. Electr. Eng. Technol., vol. 15, no. 4, pp. 1541–1554, 2020, doi: 10.1007/s42835-020-00437-2.

[13] N. Eskandarian, Y. A. Beromi, and S. Farhangi, *Improvement of Dynamic Behavior of Shunt Active Power Filter Using Fuzzy Instantaneous Power Theory*, vol. 14, no. 6, pp. 1303–1313, 2014.

[14] H. P. Thanh, H. D. Van, A. N. Duy, and C. N. Duy, *Optimizing parameters of the shunt active power filter using Genetic Algorithm*, Proc. - 2017 9th Int. Conf. Knowl. Syst. Eng. KSE 2017, vol. 2017-Janua, pp. 233–238, 2017, doi: 10.1109/KSE.2017.8119464.

[15] C. Lam and M. Wong, *Design and Control of Hybrid Active Power Filters*. 2014. [Online]. Available: http://link.springer.com/10.1007/978-3-642-41323-0

[16] Z. Chelli, R. Toufouti, A. Omeiri, and S. Saad, *Hysteresis control for shunt active power filter under unbalanced three-phase load conditions*, J. Electr. Comput. Eng., vol. 2015, 2015, doi: 10.1155/2015/391040.

[17] A. K. Mishra, S. R. Das, P. K. Ray, R. K. Mallick, A. Mohanty, and D. K. Mishra, *PSO-GWO Optimized Fractional Order PID Based Hybrid Shunt Active Power Filter for Power Quality Improvements*, IEEE Access, vol. 8, pp. 74497–74512, 2020, doi: 10.1109/ACCESS.2020.2988611.

[18] B. N. Atanga, F. B. Effah, and P. Y. Okyere, *An enhanced jumping spider optimization algorithm*, vol. 16, no. 1, pp. 46–61, 2022.

[19] M. Jamil and H. J. Zepernick, *Lévy Flights and Global Optimization*, *Swarm Intell. Bio-Inspired Comput.*, pp. 49–72, 2013, doi: 10.1016/B978-0-12-405163-8.00003-X.